Energetics of Polar Side-Chain Interactions in Helical Peptides: Salt Effects on Ion Pairs and Hydrogen Bonds†

Jeni S. Smith and J. Martin Scholtz*

Department of Medical Biochemistry and Genetics, Department of Biochemistry and Biophysics, Center for Macromolecular Design, Texas A&M University, College Station, Texas 77843-1114

Received August 14, 1997; Revised Manuscript Received October 30, 1997⊗

ABSTRACT: The energetics of the interaction between the polar side chains of glutamate or aspartate with lysine and glutamate with histidine have been determined using a model alanine-based peptide helix. An evaluation of the effects of NaCl and pH on the interactions between these acidic and basic residues in several different orientations and spacings in an α-helical peptide has been made. For many of the peptides, we find a considerable interaction between the polar side chains. In general, the shorter side chains show stronger interactions, but there are more restrictions on the precise geometry of the interactions as dictated by the spacing and orientation of the polar residues in the α-helical peptide. The energetics of the interaction between the fully-charged ion pairs can be diminished by added salt, but the interaction is not completely screened even at 2.5 M NaCl. The strength of the interaction between a charged and neutral side chain is not as sensitive to the ionic strength of the solution, suggesting that solvent-exposed hydrogen bonds are forming. All the interactions between the polar residues employed here stabilize helix formation, suggesting that solvent-exposed ion pairs and hydrogen bonds can contribute to the conformational stability of proteins and peptides.

Electrostatic ion-pair interactions influence many inter- and intramolecular interactions in biological systems. For proteins, the energetic contribution of solvent-exposed ion pairs or salt bridges (we use the term salt bridge to denote a hydrogen-bonded ion pair) to stability remains controversial. The strong attraction between charged residues is balanced by interactions of the charged groups with solvent and with other portions of the protein molecule as well as the loss of side-chain conformational entropy when the interaction is formed. For interactions buried in the interior of the protein, the evidence is clearly in favor of a stabilizing role as demonstrated by the amazing 3−5 kcal mol^{-1} that a single His-Asp ion pair contributes to the conformational stability of T4 lysozyme (*1*). Here, we address the role that solvent-exposed interactions between polar residues play in protein stability, utilizing monomeric helical peptides of defined length and sequence as models.

The energetics of helix formation for a given peptide in water is dominated by four main components: the intrinsic helix-forming tendency of each residue, specific N- and C-capping interactions, the interaction of charged side chains and the helix macrodipole, and the energetics of specific side-chain to side-chain interactions. In the simplest forms of helix to random coil theory (*2, 3*), only helix propensities (*s*- or *w*-values, respectively, for the two models) were included, ignoring interactions between different side chains and between side chains and the helix backbone. Recently, an algorithm based on the Lifson−Roig model (*3*) for the helix to random coil transition in peptides has been described (*4*). This algorithm includes additional statistical weights for side-chain interactions and can model N- and C-capping as well as the interactions between specific side chains. One of the major points of the present work is to provide the parameters that describe the energetics of the interactions between charged side chains in a helical peptide. A determination of these parameters will complement existing measures of helix propensity values and N- and C-cap parameters for these peptides (*4*). A second goal of this work is to determine if solvent-exposed ion pairs and hydrogen bonds stabilize α-helices and to compare the results from studies on helical peptides with the factors that contribute to the conformational stability of proteins.

Alanine-based peptides have provided a useful and simple model system for determining the factors that contribute to helix formation (recent reviews, refs *5*−*7*). Here we use the neutral Ala-Gln peptide (*8*) as a "host" into which we have substituted charged "guest" residues to investigate three pairs of potential side-chain interactions: Glu with Lys, Asp with Lys, and Glu with His (the remaining pair in this series, Asp with His, was reported recently, ref *9*). For each pair of guest residues, both orientations of the polar residues, with respect to the sequence in the peptide, were investigated, and the peptides have been studied at several pH values and solution conditions, including the addition of NaCl.

† Supported by grants from the National Institutes of Health (GM52483) and the Robert A. Welch Foundation (A-1281). J.M.S. is the recipient of a Junior Faculty Research Award from the American Cancer Society (JFRA-577).

* Author to whom correspondence should be addressed at the Department of Medical Biochemistry and Genetics, 440 Reynolds Building, Texas A&M University, College Station, Texas 77843-1114. Telephone: (409) 845-0828. Fax: (409) 847-9481. E-mail: jm-scholtz@tamu.edu.

⊗ Abstract published in *Advance ACS Abstracts,* December 15, 1997.

S0006-2960(97)02026-6 CCC: $15.00 © 1998 American Chemical Society
Published on Web 01/06/1998

Table 1: Sequences of the Peptides Used in This Study[a]

AQ Host	
AQ	Ac-A-A-Q-A-A-A-A-Q-A-A-A-A-Q-A-A-Y(NH$_2$)
Glu-Lys	
(i, i+3) 3EK	Ac-A-A-Q-A-A-**E**-A-Q-**K**-A-A-A-Q-A-A-Y(NH$_2$)
(i, i+4) 4EK	Ac-A-A-Q-A-A-**E**-A-Q-A-**K**-A-A-Q-A-A-Y(NH$_2$)
(i, i+5) 5EK	Ac-A-A-Q-A-A-**E**-A-Q-A-A-**K**-A-Q-A-A-Y(NH$_2$)
Lys-Glu	
(i, i+3) 3KE	Ac-A-A-Q-A-A-**K**-A-Q-**E**-A-A-A-Q-A-A-Y(NH$_2$)
(i, i+4) 4KE	Ac-A-A-Q-A-A-**K**-A-Q-A-**E**-A-A-Q-A-A-Y(NH$_2$)
(i, i+5) 5KE	Ac-A-A-Q-A-A-**K**-A-Q-A-A-**E**-A-Q-A-A-Y(NH$_2$)
Asp-Lys	
(i, i+3) 3DK	Ac-A-A-Q-A-A-**D**-A-Q-**K**-A-A-A-Q-A-A-Y(NH$_2$)
(i, i+4) 4DK	Ac-A-A-Q-A-A-**D**-A-Q-A-**K**-A-A-Q-A-A-Y(NH$_2$)
(i, i+5) 5DK	Ac-A-A-Q-A-A-**D**-A-Q-A-A-**K**-A-Q-A-A-Y(NH$_2$)
Lys-Asp	
(i, i+3) 3KD	Ac-A-A-Q-A-A-**K**-A-Q-**D**-A-A-A-Q-A-A-Y(NH$_2$)
(i, i+4) 4KD	Ac-A-A-Q-A-A-**K**-A-Q-A-**D**-A-A-Q-A-A-Y(NH$_2$)
(i, i+5) 5KD	Ac-A-A-Q-A-A-**K**-A-Q-A-A-**D**-A-Q-A-A-Y(NH$_2$)
Glu-His	
(i, i+3) 3EH	Ac-A-A-Q-A-A-**E**-A-Q-**H**-A-A-A-Q-A-A-Y(NH$_2$)
(i, i+4) 4EH	Ac-A-A-Q-A-A-**E**-A-Q-A-**H**-A-A-Q-A-A-Y(NH$_2$)
(i, i+5) 5EH	Ac-A-A-Q-A-A-**E**-A-Q-A-A-**H**-A-Q-A-A-Y(NH$_2$)
His-Glu	
(i, i+3) 3HE	Ac-A-A-Q-A-A-**H**-A-Q-**E**-A-A-A-Q-A-A-Y(NH$_2$)
(i, i+4) 4HE	Ac-A-A-Q-A-A-**H**-A-Q-A-**E**-A-A-Q-A-A-Y(NH$_2$)
(i, i+5) 5HE	Ac-A-A-Q-A-A-**H**-A-Q-A-A-**E**-A-Q-A-A-Y(NH$_2$)

[a] The peptides are *N*-acetylated (Ac) and the α-carboxyl group is amidated (NH_2) to eliminate free charges at the helix termini. The peptides are abbreviated as shown with the number indicating the spacing between residues, and the order of the charged residues indicates the orientation with respect to the sequence of the peptide.

MATERIALS AND METHODS

Peptide Synthesis, Purification, and Characterization. The peptides (Table 1) were synthesized by solid-phase peptide synthesis methods using FMOC chemistry (*10*, *11*). The amino acid residues used were either activated esters or free acids, and coupling was facilitated by the use of HBTU (*O*-benzotriazole-*N*,*N*,*N*′,*N*′-tetramethyluronium hexafluorophosphate) and HOBt (*N*-hydroxybenzotriazole). The N- and C-termini of each peptide are blocked with acetyl and carboxyamide, respectively. Cleavage of the peptide from the resin and removal of the side-chain protecting groups was performed with trifluoroacetic acid (TFA) and the cation scavenger anisole. The peptides were then precipitated in ether, dissolved in water, and lyophilized. The peptides were purified on a reverse-phase column with C_{18} resin using fast performance liquid chromatography (FPLC).

The mass of each peptide was confirmed using matrix-assisted laser desorption-ionization (MALDI) time-of-flight mass spectroscopy with α-cyano-4-hydroxycinnamic acid as the matrix. Peptide purity was verified by analytical FPLC (C_{18} column) and was found to be ≥95%. Stock solutions of each peptide were made fresh daily; the concentration of the stock solution in water was determined from the absorbance of the single tyrosine residue at 275 nm, using an extinction coefficient of 1.39 mM^{-1} cm^{-1} (*12*). The absorbance was measured with a Cary 219 UV/VIS spectrophotometer.

Determination of Helical Content in Each Peptide. Ellipticity at 222 nm was measured on an AVIV model 62 DS circular dichroism (CD)[1] spectrophotometer equipped with a temperature-controlled cell and a stirring unit. The instrument was calibrated with (+)-10-camphorsulfonic acid, and all data are reported as mean residue ellipticity, $[\theta]_{222}$ (deg cm^2 $dmol^{-1}$). The wavelength spectra were determined at 0 °C in 3 mM potassium fluoride and 10 mM potassium phosphate buffers. The effects of different concentrations of sodium chloride at neutral, acidic, and basic conditions were measured by preparing individual samples at each salt concentration and pH in CD buffer (1 mM each of sodium borate, sodium citrate, and sodium phosphate). The Asp-Lys (DK) or Glu-Lys (EK) peptides were prepared in pH 7.0 (D^-K^+ or E^-K^+) and pH 2.5 (D^0K^+ or E^0K^+) buffer, and the Glu-His series was prepared in pH 8.5 (E^-H^0), pH 5.5 (E^-H^+), and pH 2.5 (E^0H^+) buffer. Samples were prepared individually and in triplicate.

Data Analysis. The helical content of the peptides in various solutions was monitored at 222 nm by circular dichroism, and the fraction of helix for each peptide was calculated from the mean residue ellipticity (deg cm^2 $dmol^{-1}$) using

$$f_H = \frac{[\theta]_{obs} - [\theta]_C}{[\theta]_H - [\theta]_C} \quad (1)$$

where the values for the complete random coil and the chain-length dependent full helix are

$$[\theta]_C = +640 \text{ deg cm}^2 \text{ dmol}^{-1} \quad (2)$$

$$[\theta]_H = -42500(1 - 3/n) \text{ deg cm}^2 \text{ dmol}^{-1} \quad (3)$$

where $n = 16$, the number of residues with flanking amide groups in each peptide (*13*). These values are identical to those used previously to determine the helix propagation parameters in related alanine-based peptides (*4*).

To determine the separate energetic components to helix formation in these peptides, the helicity data were analyzed with a modified Lifson−Roig helix−coil transition theory (*4*, *14*). The modification allows us to separate the energetics of side-chain interactions from the other contributions to helix formation in these peptides. For the analysis of each peptide,

[1] Abbreviations: CD, circular dichroism; ΔG_{sc}, Gibbs free energy change for the side-chain interaction; $\langle w_{AQ} \rangle$, average helix propagation parameter for the AQ host peptide; w_X, *w*-value for amino acid residue X.

Table 2: Lifson−Roig Helix−Coil Parameters for These Peptides[a]

residue	*w*-value(s)	N-cap	C-cap
$\langle AQ \rangle_{favorable}$[b]	1.35, 1.38, 1.37	1.0	1.0
$\langle AQ \rangle_{unfavorable}$[c]	1.30, 1.36, 1.35	1.0	1.0
Asp^0	0.40	1.0	1.0
Asp^-	0.38	6.6	1.0
Glu^0	0.70	1.0	1.0
Glu^-	0.54	2.06	1.0
His^0	0.36	2.12	1.0
His^+	0.22	1.0	1.0
Lys^+	1.00	0.72	1.0

[a] Parameters used in the analysis of the data. The Lifson−Roig formalism of helix−coil theory has been used as implemented in the computer program *helix2*, written by Carol Rohl (*4*, *14*). The data used to determine the parameters for the charged residues are summarized in Rohl et al. (*4*). We have used a constant nucleation parameter (v = 0.036) for all residues (*4*). [b] The Ala-Gln host peptide is treated as a homopolymer. The average $\langle w_{AQ} \rangle$ is the best-fit parameter for the set of peptides with at least one favorable charge−dipole interaction. The three $\langle w_{AQ} \rangle$ values are for the data sets in 0.01, 1.0, and 2.5 M NaCl, respectively. [c] The Ala-Gln host peptide is treated as a homopolymer. The average $\langle w_{AQ} \rangle$ is the best-fit parameter for the set of peptides with at least one unfavorable charge−dipole interaction. The three $\langle w_{AQ} \rangle$ values are for the data sets in 0.01, 1.0, and 2.5 M NaCl, respectively.

we employ three helix propagation parameters, one for the Ala-Gln host, $\langle w_{AQ} \rangle$, and one each for the two guest residues. We use a common helix nucleation parameter (v) for all residues, and we also use the recently determined N- and C-cap parameters for the guest residues (*4*). The values for all the parameters used in this analysis are collected in Table 2. The reference peptides (i, i+5) with the same amino acid composition as the peptides with potential interactions are used to determine the average propagation parameter $\langle w_{AQ} \rangle$ of the helix under given solvent conditions. This average $\langle w_{AQ} \rangle$ value incorporates any other energetic components that are not included in the normal propagation parameters (*w*-values) or capping parameters (N- and C-cap values). Since these peptides have residues with charged side chains, these additional interactions include the interactions of the charged side chains with the helix macrodipole (*15*−*18*). In our treatment, these charge−dipole effects are included in two ways: one is in the N-cap parameters for the individual charged residue as originally suggested (*19*, *20*) and also, we have allowed the *w*-values for the host residues $\langle w_{AQ} \rangle$ to change for the two different classes of peptides employed. While the first correction is specific for a given residue, the latter depends only on the charge(s) on the side chain(s). We exploit this latter phenomenon by grouping the peptides into two classes, one with at least one favorable charge−dipole interaction (Glu^-−His^+, for example) and the second set with at least one unfavorable charge−dipole interaction (His^+−Glu^-, for example). A common $\langle w_{AQ} \rangle$ value for each of the two classes of data is determined, through a nonlinear least-squares analysis of the data for the reference peptides (the AQ host and the (i, i+5) peptides). This classification and fitting procedure also allows us to adequately describe the effects of salts (or, in general terms, the ionic strength of the solution) for all the solution conditions investigated (see below).

The final key aspect to the new modification of the Lifson−Roig model for the helix−coil transition is the incorporation of specific side-chain interactions to the partition function for the system (*4*, *14*, *17*). These additional statistical weights reflect the energetic contribution of a specific side-chain interaction to helix formation. The two new statistical weights, p and q, are defined as the equilibrium constants for the formation of (i, i+4) and (i, i+3) side-chain interactions, respectively, such that

$$\Delta G_{(i,i+4)} = -RT \ln(p) \quad (4)$$

$$\Delta G_{(i,i+3)} = -RT \ln(q) \quad (5)$$

These statistical weights contribute to the partition function only when the interacting residues and all intervening residues are in the helical state. The Gibbs free energy changes, as defined by eqs 4 and 5, thus represent the contributions of the specific side-chain interaction to the stability of the full helix. These definitions of ΔG_{sc}, the interaction free energy between the side chains, provide measures of the strength of the interaction in the fully helical state. Alternative methods for calculating ΔG_{sc}, as from apparent pK_a shifts of the interacting residues, capture the population weighted average pK_a of the helical and coiled residues. ΔG Values of calculated from apparent pK_a shifts are thus lower than those determined from eqs 4 and 5 because of the multistate nature of the helix to coil transition. This point has been discussed previously (*9*). Furthermore, the magnitude of apparent pK_a shift measured on the population of molecules will depend upon the total helicity of the population, thus making comparisons between different peptides and pairs of side chains difficult. Since we are interested in the stabilization afforded by polar side-chain interactions in helical conformation, we use eqs 4 and 5 to determine the energetics of the interaction. The new computer program *helix2*, by Carol Rohl (*4*, *14*), contains these modifications of Lifson−Roig helix−coil transition theory. Further information about this program is available (*4*). Here, we use this program to determine p- and q-values for the polar side-chain interactions between Glu-Lys, Asp-Lys, and Glu-His. The remaining pair, Asp-His, is the subject of another recent report (*9*).

The nonlinear least-squares fitting procedures were performed using the modified Gauss−Newton nonlinear function minimization program NONLIN (*21*, *22*) on a Silicon Graphics Indigo computer. The largest source of error in these experiments is in the measure of $[\theta]_{222}$, and we estimate it to be ±3−4% on a single measurement. To determine how these errors propagate to the final ΔG_{sc} values, we performed fits of the experimental data where we introduced a 3% error in $[\theta]_{222}$; the reported uncertainties in ΔG_{sc} reflect this approach.

RESULTS

Peptide Design and Characterization of Helical Structure. The peptides employed here (Table 1) are derivatives of the neutral Ala-Gln host peptide (*8*) where the high helix-forming tendency of Ala affords helical structure (*23*), and the three Gln residues, spaced (i, i+5), provide water solubility. This peptide serves as the host, into which we have substituted pairs of polar residues at positions 6 and 9, 10 or 11, to provide (i, i+3), (i, i+4), and (i, i+5) potential interactions (see Table 1 for the sequences and naming scheme). The guest sites have been selected so as to place the potential interaction in the center of the peptide, where helix content is higher, end effects are minimized, and potential interac-

Table 3: Observed Helicity ($-[\theta]_{222}$ in deg cm^2 dmol^{-1}) of Each of the Peptides at 0 °C[a]

	0.01 M NaCl			1.0 M NaCl			2.5 M NaCl		
peptide	*i*, *i*+3	*i*, *i*+4	*i*, *i*+5	*i*, *i*+3	*i*, *i*+4	*i*, *i*+5	*i*, *i*+3	*i*, *i*+4	*i*, *i*+5
E^0K^+	10700	12100	9800	12450	14150	11100	12750	13450	10600
E^-K^+	11400	12750	8500	11750	13100	9700	11050	12100	9200
D^0K^+	7700	8500	6900	7900	9500	8000	7500	8700	7600
D^-K^+	8200	9200	7400	8900	10000	8400	8000	8900	8000
E^0H^+	4200	3900	4400	4800	4500	5100	4000	4300	4800
E^-H^+	4500	4100	3600	5000	4400	4300	4400	4000	4000
E^-H^0	5100	4400	4700	5600	5100	5500	4700	4900	5200
AQ host[b]		15580			16580			15250	
K^+E^0	10050	9700	7900	12100	11050	10400	11750	11400	9900
K^+E^-	9000	10350	6900	10350	10700	9100	8650	8650	8700
K^+D^0	7800	8100	5900	9600	10100	7900	8600	8700	7500
K^+D^-	8400	10300	5800	8400	10100	7700	7400	8700	7300
H^+E^0	5100	5400	2700	5700	5900	3900	4500	4500	3700
H^+E^-	4400	5300	2300	5000	5300	3300	4100	4300	3100
H^0E^-	3300	3300	3400	6400	6600	4700	5200	5400	4500

[a] For each orientation and charged state of the polar residues, data are provided for the three different spacings at each of the three concentrations of NaCl. The entries for Glu^0 or Asp^0 with Lys^+ were determined at pH 2.5, while those for the full ion pair (Glu^- or Asp^- with Lys^+) are at pH 7.0. The Glu-His data were measured at pH 2.5 (Glu^0-His^+), pH 5.5 (Glu^--His^+), or pH 8.5 (Glu^--His^0). The ionization state on the charged residue is given by a superscript (0/+/−). [b] The host peptide has no guest residues and is arbitrarily listed under the (*i*, *i*+4) column. The peptides listed above the host all contain at least one favorable charge−helix macrodipole interaction and those listed after the host have at least one unfavorable charge−helix macrodipole interaction. See the text for details.

tions with a host Gln residue are avoided (*16*, *17*). Since the α-helix has 3.6 residues per turn, we expect helix-stabilizing interactions at (*i*, *i*+3) and (*i*, *i*+4) spacings; the (*i*, *i*+5) peptides are designed to be reference peptides and should not show any helix-stabilizing side-chain interactions. The peptides in the Glu-Lys series have been described before (*17*). We include them here and have re-analyzed the data with the full model for the helix−coil transition and the revised parameters for the new model. By including these data, we can also provide a quantitative comparison between the energetics of the interaction between different pairs of polar residues.

The CD spectra of the Asp-Lys, Glu-Lys, and the Glu-His peptides all show the double minima typical of helical secondary structure (data not shown). Each peptide shows an isodichroic point at ≈203 nm in the spectra when the amount of helix is altered by either raising the temperature or adding a helix-stabilizing solvent additive like trifluoroethanol (data not shown). The isodichroic point is consistent with each residue existing in either a helical conformation or a random coil, with no alternative structures throughout the transition. It is important to realize that the presence of an isodichroic point does not imply that helix formation in these peptides follows a two-state reaction at the level of the entire chain. For these alanine-based peptides, the non-two-state behavior of helix formation has been firmly established (*24*, *25*). Fortunately, helix−coil theory has been shown to describe helix formation in these peptides (*13*, *26*−*31*). The parameters used in Table 2 for the analysis of helix formation in these peptides have been determined previously from related alanine-based peptides. Therefore, the parameters (Table 2) that govern helix formation in the absence of specific side-chain interactions have been determined using similar peptides, and these parameters have been shown to adequately describe helix formation in these and related peptides (*4*).

The helix contents of the peptides are listed in Table 3 and shown in Figure 1. Each peptide with guest residues is less helical than the host peptide, reflecting the differences in *w*-values between the host and guest residues (Table 2). This is especially evident in a comparison of the reference (*i*, *i*+5) peptides, where we do not expect to see helix-stabilizing side-chain interactions. For a given salt concentration, the AQ host peptide is always the most helical, and the substitution of a guest residue can have a dramatic effect on helix content, up to 2-fold in some cases.

In comparing the different sets of peptides, the general trend in helicity is Glu-Lys > Asp-Lys > Glu-His. This is easy to reconcile from the known helix propensity values for the guest residues (Table 2). In comparing the Glu-Lys and Asp-Lys peptides, the *w*-value for Glu is larger than the *w*-value for Asp, hence the Glu-Lys peptides are more helical than the Asp-Lys peptides. The same general result is observed in comparing the Glu-Lys and Glu-His peptides; Lys has a higher *w*-value than His, hence the Glu-Lys peptides are more helical that the Glu-His peptides.

Effects of NaCl on Helix Formation. Since we are exploring interactions between side chains with at least one, and sometimes two, charged side chains, we have investigated the effects of NaCl on helix formation in the peptides. Table 3 and Figure 1 show the observed helicity of each combination of charged residues at three different concentrations of NaCl: 0.01, 1.0, and 2.5 M. As expected, the helical contents of the peptides are altered by changes in solvent composition. The effects of salt on the AQ host peptide have been described before (*8*). In this neutral host peptide, the helicity increases up to 1 M NaCl, due to screening of the helix macrodipole. Beyond 1 M NaCl, helicity decreases as expected from the Hofmeister effect (see ref *8* for details and discussion). The effects of ionic strength on helix formation in the other peptides is composed of three main components: the screening of the neutral helix macrodipole illustrated by the AQ host peptide, the interaction of charged side chains with the helix macrodipole, and the interactions between charged side chains. Since we are interested in quantifying the latter, we must remove contributions from the first two effects. We have used a simple approach to this problem, utilizing the changes in helix contents of the

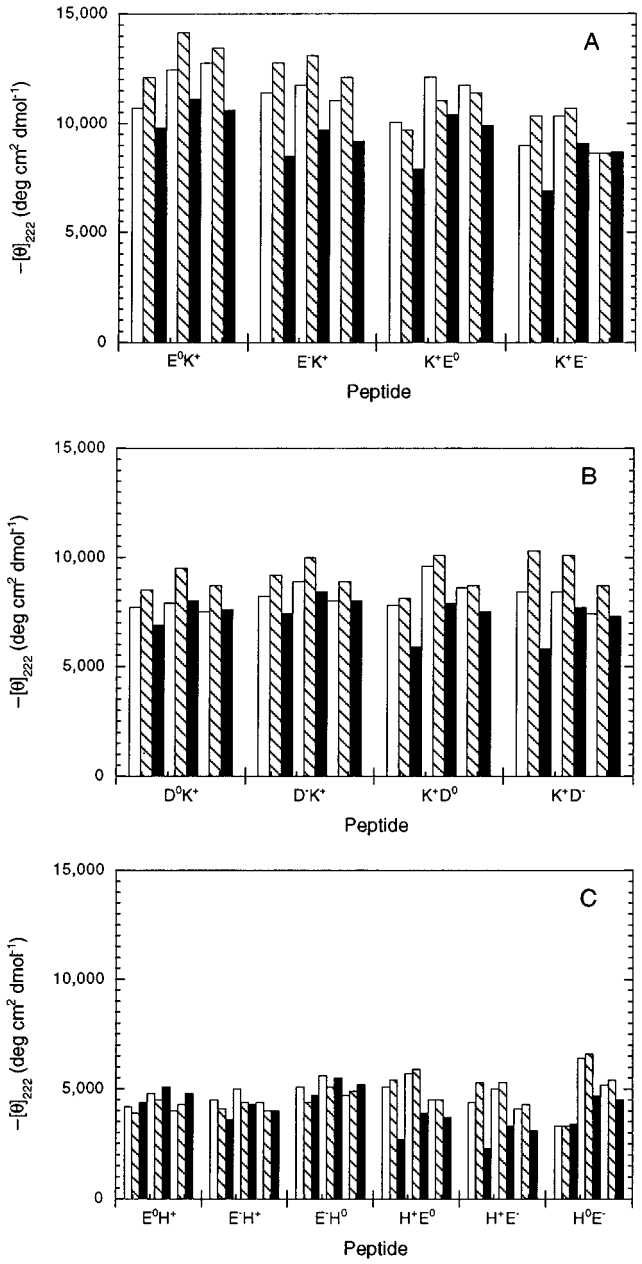

FIGURE 1: Observed helicity for the peptides employed in this study. In Panel A are the Glu-Lys peptides with the ionization state of the residues and the orientation of the Glu and Lys residues indicated. Within each group is shown the data obtained in 0.01 M NaCl, 1.0 M NaCl, and 2.5 M NaCl (reading from left to right) for the (*i*, *i*+3) (open bars), (*i*, *i*+4) (hatched bars), and (*i*, *i*+5) (solid bars) spacings of the indicated residues. Panels B and C show the same data in the identical format for the Asp-Lys and Glu-His peptides, respectively.

reference (*i*, *i*+5) peptides and the AQ host with ionic strength to determine the contributions of the first two effects without introducing additional complexity to helix−coil theory. The charge−macrodipole interactions are handled in two ways: one is to incorporate the N- and C-cap parameters as originally suggested (*19*, *20*) as a way to localize the charged residues at given positions in the helical peptide. The other is to use two different average helix propagation parameters for the host residues, $\langle w_{AQ} \rangle$, for the two "classes" of peptides. For the peptides listed above, the host peptide in Table 3, the charged guest residues are oriented such that there is at least one (and sometimes two)

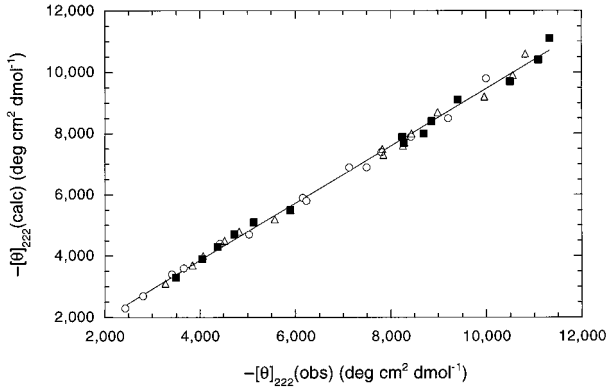

FIGURE 2: Observed and calculated helicity for the reference (*i*, *i*+5) peptides used in this study at the three different concentrations of NaCl employed: (○), 0.01 M; (■), 1.0 M; (△), 2.5 M. The calculated helicity employed the parameters listed in Table 2 and the full treatment of the modified Lifson−Roig model for the helix to random coil transition in peptides (*4*).

favorable interactions with the helix macrodipole. We group these together in the "favorable" class and determine $\langle w_{AQ} \rangle_{favorable}$. The "unfavorable" class includes those peptides below the AQ host in Table 3 and is used to determine $\langle w_{AQ} \rangle_{unfavorable}$ in a similar fashion.

The analyses of the two sets of data, the favorable and unfavorable sets, proceeds as follows at each of the three concentrations of salt. For each reference peptide in the set, the AQ host, and the (*i*, *i*+5) peptides, we employ three propagation (*w*) parameters: one for each of the two guest residues (Table 2) and one common parameter for the host residues (w_{AQ}). We also use a fixed nucleation parameter (υ) and the N- and C-cap parameters for the guest residues listed in Table 2. This allows us to find the best-fit values for w_{AQ}. These are shown in Table 2. Figure 2 shows the comparison of the observed and calculated helicity for each reference peptide using the determined parameters. The excellent agreement means that we have captured the electrostatic interactions between a charged side chain and the helix macrodipole in the fashion described.

Having successfully modeled the nonspecific interactions between a charged side chain and the helix macrodipole, we can now apply the parameters in Table 2 to determine the energetics of side-chain interactions in the (*i*, *i*+3) and (*i*, *i*+4) peptides. If the charged side chains do not affect helix stabilization, the parameters in Table 2 should be sufficient to predict the helix content of all the peptides. Conversely, if there is an interaction between the two guest residue side chains, we can quantify the energetics (ΔG_{sc}) through the use of eqs 4 and 5, respectively, for the (*i*, *i*+3) and (*i*, *i*+4) spacings. The results are shown in Table 4 for all the peptides at each concentration of NaCl. The magnitude of the side-chain interaction energy ranges from 0 to 650 cal mol^{-1} with no NaCl and from 0 to 270 cal mol^{-1} at 2.5 M NaCl. Figure 3 illustrates the differences in side-chain interaction energy for the different peptides and shows how ΔG_{sc} decreases at higher ionic strength.

DISCUSSION

Simple α-helical peptides of defined sequence and length are excellent models for investigating specific interactions that are important in biological systems, like ion pairs and hydrogen bonds. Our peptides also have the advantage that

Table 4: Energetics of the Side-Chain Interactions at 0 °C[a]

	0.01 M NaCl		1.0 M NaCl		2.5 M NaCl	
interaction	*i*, *i*+3	*i*, *i*+4	*i*, *i*+3	*i*, *i*+4	*i*, *i*+3	*i*, *i*+4
E^0K^+	100	220	130	275	190	255
E^-K^+	290	415	200	320	180	270
D^0K^+	100	180	0	160	0	120
D^-K^+	120	240	80	200	0	120
E^0H^+	120	0	90	0	0	0
E^-H^+	300	190	270	120	200	80
E^-H^0	150	0	100	0	50	0
K^+E^0	235	200	185	80	185	160
K^+E^-	280	400	175	180	30	30
K^+D^0	320	390	260	280	190	180
K^+D^-	400	580	150	320	80	210
H^+E^0	480	520	320	340	180	170
H^+E^-	500	650	350	340	180	170
H^0E^-	390	430	280	300	160	180

[a] For each orientation and charged state of the polar residues, ΔG_{sc} values (cal mol^{-1}) are provided for the two different spacings at each of the three concentrations of NaCl. Positive values of ΔG_{sc} indicate stabilizing interactions. The error on each ΔG measurement ranges from ± 50 to ± 80 cal mol^{-1}. The entries for Glu^0 or Asp^0 with Lys^+ were determined at pH 2.5, while those for the full ion pair (Glu^- or Asp^- with Lys^+) were determined at pH 7.0. The Glu-His data were measured at pH 2.5 (Glu^0-His^+), pH 5.5 (Glu^--His^+), or pH 8.5 (Glu^--His^0). The ionization state on the charged residue is given by a superscript (0/+/−).

the host peptide is uncharged, and thus the interactions between guest residues with charged side chains can be investigated without the potential complications of the guest residues interacting with other charges in the host peptide. The host peptide is also well-suited for these studies because it shows approximately 50% helix, and thus perturbations of the amount of helical structure present can be easily measured by far-UV circular dichroism. Helix formation in these alanine-based peptides and other simple peptides is also described well by helix−coil transition theory, and the basic framework of the models has been adapted to include other helix-stabilizing interactions, such as the ion-pair and hydrogen-bonding interactions investigated here.

Our results show that solvent-exposed polar interactions can contribute to the conformational stability of peptides and, hence, proteins. All pairs of polar residues investigated here are capable of forming a stabilizing interaction in at least one orientation and spacing in the α-helix. Together with the recent report on the His-Asp pair (*9*), we now have a complete accounting of the energetics of ion-pair and hydrogen-bonding interactions for Asp and Glu with Lys or His in helical peptides. These data, along with the recent determination of residue helix propensities and N-capping parameters (*4*, *32*), can now be used to predict the helix content of any alanine-based peptide using the available model for the helix to random coil transition.

There are several factors that contribute to α-helix formation in our simple alanine-based model peptides, and these factors govern the amount of helical structure we observe (Table 3). For the peptides employed here, where we have substituted a pair of polar residues for alanine residues near the center of the sequence, there are two main considerations. These are the differences in intrinsic helix-forming tendency (helix propensity) between the polar guest residues and alanine (*w*-values) and the possible interaction energy between the polar side chains of the guest residues. The major contribution between these two effects on the

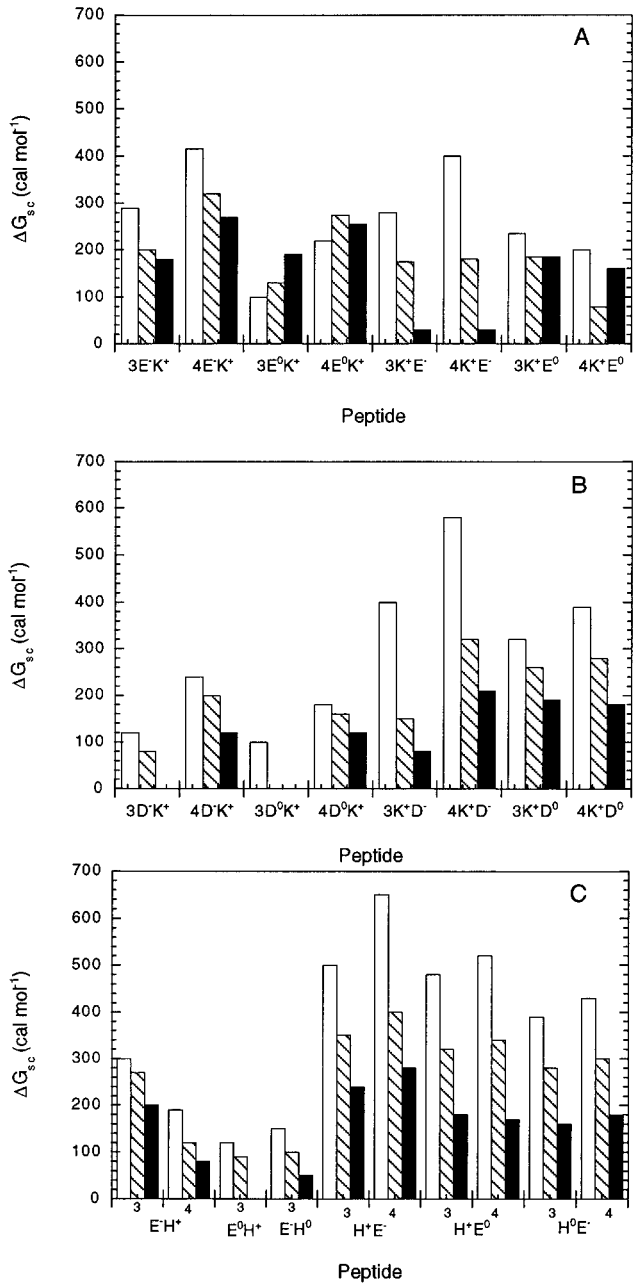

FIGURE 3: The energetics of the measured interaction between the side chains is shown for the Glu-Lys (A), Asp-Lys (B), and Glu-His (C) peptides at 0 M NaCl (open bars), 1.0 M NaCl (hatched bars), and 2.5 M NaCl (solid bars). Here, positive values of ΔG_{sc} indicate a stabilizing interaction. Each peptide is labeled with the spacing (3 or 4) between the two residues, the orientation of the two side chains in the sequence, and the ionization state for that side chain. For some of the peptides under some salt concentration, the measured ΔG_{sc} is zero (see Table 4).

observed helicity of the peptides is the first factor—all the polar residues have lower *w*-values than alanine in the host peptide (Table 2), hence all the peptides are less helical than the host peptide. This is most easily seen in comparing the reference (*i*, *i*+5) peptides, where no side-chain interactions are possible, with the AQ host (Table 3). For these reference peptides, we find the *w*-values for the individual guest residues are sufficient to calculate the expected helicity for each reference peptide (Figure 2), indicating that the *w*-values for the polar residues (Table 2) and our application of the new helix−coil model (*4*) are justified. This is important

since the model employed and the *w*-value parameters derived from it were determined with alanine-based peptides. Our results clearly indicate (Figure 2) that this model, with these parameters, can adequately describe helix formation in alanine-based peptides.

The α-helix has 3.6 residues per turn, so peptides with (*i*, *i*+3) and (*i*, *i*+4) spacings of polar residues are capable of exhibiting side-chain interactions. In comparing the helix contents of the (*i*, *i*+3) and (*i*, *i*+4) peptides with the (*i*, *i*+5) reference peptides (Table 3 and Figure 1), it is clear that most combinations of polar groups do show an increase in the amount of helical structure above that observed for the corresponding reference peptide. This increase in helicity has been used to quantify the energetics of the side-chain interaction to afford a measure of ΔG_{sc} for each pair of polar residues at different values of pH and various concentrations of NaCl. The ΔG_{sc} values are collected in Table 4 and shown in Figure 3. In general, the ΔG_{sc} values are quite modest, ranging from 0 to 650 cal mol^{-1}. This range in energy is comparable to the differences in ΔG for helix propensity, since the range for alanine (the best helix former) to glycine (one of the worst helix formers) is only about 1 kcal mol^{-1} (*33*, *34*). Therefore, the modest ΔG_{sc} values can make a large contribution to the observed helicity of the peptides, as reflected in the measured ellipticity values (Table 3).

The ionic strength of the solution does have a measurable effect on the ΔG_{sc} values for the interaction, as expected for solvent-exposed interactions between side chains with either one or two formal charges. For the peptides with both residues in their charged forms, ΔG_{sc} values are more favorable at low salt concentration, and the strength of the side-chain interaction diminishes, but does not vanish, with increasing NaCl concentration. In contrast, the effects of NaCl on the peptides with only one charged residue in the pair are more variable and the changes in ΔG_{sc} with increasing NaCl are more modest. Together, these results suggest that the a major factor in the interaction between these side chains is hydrogen bonding and that the interaction observed in the full ion pairs at high salt is not just a simple electrostatic interaction. This point is best illustrated by comparing two peptides at different pH values, like the $4E^-K^+$ and $4E^0K^+$ pairs. At low ionic strength the peptide with the full ion pair, $4E^-K^+$, has a more favorable ΔG_{sc} than the peptide with the singly-charged hydrogen bond, $4E^0K^+$; however, at high ionic strength the ΔG_{sc} values are nearly identical. Hence, a major component of the interaction between Glu and Lys cannot be screened by external salts, consistent with a role for hydrogen bonding in these interactions (*17*).

The other major conclusion from our results is that shorter side chains, in general, have larger ΔG_{sc} values than residues with longer side chains, although there are more restrictions on the spacing and orientations of residues within the helix with shorter side chains. These restrictions can be understood by considering the geometry of the α-helix: in the preferred rotamer conformation, the $C_\alpha-C_\beta$ bond vector points toward the N-terminus in a helix since there are steric clashes between non-hydrogen atoms on Cγ and the backbone CO group in the *trans* χ_1 rotamer. The preferred χ_1 conformation for shorter side chains is thus the *gauche*$^+$ rotamer, and this limits close contact with side chains that are C-terminal, even at appropriate spacings for the α-helix. While this effect is seen in the Asp-Lys and Lys-Asp peptides (Figure 3), it is best illustrated through a comparison of the His-Glu peptides with those for His and Asp reported previously (*9*). For the interaction between Glu and His, there are measurable interactions for both orientations of the polar residues (Table 4 and Figure 3), with the His-Glu orientation preferred. Also, there are only small differences between the (*i*, *i*+3) and (*i*, *i*+4) spacings, especially in the His-Glu orientation. This is in contrast to the results for the interaction between Asp and His where only the His-Asp orientation provides a helix-stabilizing side-chain interaction and the (*i*, *i*+4) spacing is preferred over the (*i*, *i*+3) peptides (*9*). The shorter acidic side chain makes a much stronger interaction when it is C-terminal to the basic (or neutral) partner.

Comparisons to Other Systems. Our results indicate that interactions between solvent-exposed, conformationally flexible polar side chains can provide measurable stability to α-helical peptides, and hence proteins. This result is in accord with previous studies of the role of ion-pair formation in other helical peptide models (*9*, *17*, *35*−*38*). In several of these previous studies, it was not possible to separate cleanly the energetics of the polar side-chain interactions from the other factors that contribute to helix formation in small peptides. Our design strategy and data analysis techniques enable us to do this, and we have now measured the energetics for an entire set of polar side-chain interactions.

Our results agree well with other quantitative measures of the strength of a Glu-Lys ion pair (ca. 500 cal mol^{-1}) reported previously (*17*, *36*) and the qualitative order provided for the other pairs (*35*, *37*, *38*) reported in α-helical peptides. Recently, there has been a report using a *β*-sheet in a zinc finger peptide as a model to investigate the energetics of ion-pair formation in water (*39*). The results from that study are in good agreement with the present results: a solvent-exposed ion pair is stabilizing up to about 500 cal mol^{-1} at low ionic strength. Furthermore, Blasie and Berg (*39*) find that salt (NaCl) can alter the energetics of ion-pair formation in the *β*-sheet peptide, similar to what we find here. Therefore, the energetics determined here for a solvent-exposed ion-pair interaction are not unique to the α-helix and should be applicable to the general question of protein stability.

The role of hydrogen bonding in protein stability remains one of the most controversial subjects in modern biochemistry. The experimental evidence seems clearly in favor of hydrogen bonds being stabilizing (for a recent review, see ref *40*), yet theoretical studies often reach the opposite conclusion (*41*, *42*). Since the interactions studied here clearly have hydrogen bonding as a major component, it is worth comparing our results to experimental studies of hydrogen bonding in proteins. Most studies of hydrogen bonding in proteins investigate buried hydrogen bonding groups. There are several important and distinct differences between buried and solvent-exposed hydrogen bonds that need to be considered. First, hydrogen bonds buried in the interior of a protein are in an environment with a dielectric constant lower than that of water and therefore should be enthalpically stronger. Second, buried hydrogen bonds in proteins involve groups that are more conformationally fixed and hence entropically favored over solvent-exposed, po-

tentially mobile side chains in an α-helix. Third, the polar groups comprising buried hydrogen bonds in proteins must be desolvated when placing them in the interior of a protein; this unfavorable desolvation penalty is not necessary for solvent-exposed interactions. Fourth, protein interiors are tightly packed, and thus favorable van der Waals interactions can stabilize polar groups to a larger extent when buried relative to solvent-exposed positions. Since the relative contributions of these four major effects are different for buried and solvent-exposed hydrogen bonds, it is not surprising that experimental studies on hydrogen bonding in proteins, which places ΔG for an intramolecular hydrogen at 1−2 kcal mol^{-1}, and our results in the α-helical peptides with a smaller range of 0.2−0.6 kcal mol^{-1} are not in perfect quantitative agreement. However, the general conclusion is the same: hydrogen bonding and other polar interactions do make favorable contributions to the conformational stability of peptides and proteins, both at buried and solvent-exposed positions.

In conclusion, we have shown that the use of model peptides and the perturbation of the equilibrium between helix and random coil is a good way to determine the energetics of specific side-chain interactions through a comparison of peptides with identical composition, but different spacings of the polar residues. Polar side-chain interactions can stabilize the helical conformation of these peptides and increase helical content, even though the measured ΔG_{sc} values are quite modest, ranging from 0 to 0.65 kcal mol^{-1} for the pairs of residues. The ΔG_{sc} values vary for the different pairs of residues and different spacings, and in general we find that residues with shorter side chains make stronger interactions. However, the geometric constraints, in terms of spacing and orientation, are more restrictive for residues with shorter side chains than for those residues with longer side chains. Finally, solvent-exposed polar side-chain interactions do make favorable contributions to peptide, and hence protein, stability.

ACKNOWLEDGMENT

We thank Drs. Robert Baldwin, Andrew Doig, Beatrice Huyghues-Despointes, Nick Pace, and Carol Rohl for helpful discussions, assistance in data analysis, and preprints of their recent articles.

REFERENCES

1. Anderson, D. E., Becktel, W. J., and Dahlquist, F. W. (1990) *Biochemistry 29*, 2403−2408.
2. Zimm, B. H., and Bragg, J. K. (1959) *J. Chem. Phys. 31*, 526−535.
3. Lifson, S., and Roig, A. (1961) *J. Chem. Phys. 34*, 1963−1974.
4. Rohl, C. R., Chakrabartty, A., and Baldwin, R. L. (1996) *Protein Sci. 5*, 2623−2637.
5. Scholtz, J. M., and Baldwin, R. L. (1995) in *Peptides: Synthesis, Structures, and Applications*, pp 171−192, Academic Press, San Diego.
6. Chakrabartty, A., and Baldwin, R. L. (1995) *Adv. Protein Chem. 46*, 141−176.
7. Kallenbach, N. R., Lyu, P., and Zhou, H. (1996) in *Circular Dichroism and the Conformational Analysis of Biopolymers*, pp 201−259, Plenum Press, New York.
8. Scholtz, J. M., York, E. J., Stewart, J. M., and Baldwin, R. L. (1991) *J. Am. Chem. Soc. 113*, 5102−5104.
9. Huyghues-Despointes, B. M. P., and Baldwin, R. L. (1997) *Biochemistry 36*, 1965−1970.
10. Atherton, E., and Sheppard, R. C. (1985) *J. Chem. Soc., Chem. Commun. 3*, 165−166.
11. Fields, G. B., and Noble, R. L. (1990) *Int. J. Pept. Protein Res. 35*, 161−214.
12. Brandts, J. R., and Kaplan, L. J. (1973) *Biochemistry 12*, 2011−2024.
13. Scholtz, J. M., Qian, H., York, E. J., Stewart, J. M., and Baldwin, R. L. (1991) *Biopolymers 31*, 1463−1470.
14. Stapley, B. J., Rohl, C. A., and Doig, A. J. (1995) *Protein Sci. 4*, 2383−2391.
15. Shoemaker, K. R., Kim, P. S., Brems, D. N., Marqusee, S., York, E. J., Chaiken, I. M., Stewart, J. M., and Baldwin, R. L. (1985) *Proc. Natl. Acad. Sci. U.S.A. 82*, 2349−2353.
16. Huyghues-Despointes, B. M. P., Scholtz, J. M., and Baldwin, R. L. (1993) *Protein Sci. 2*, 1604−1611.
17. Scholtz, J. M., Qian, H., Robbins, V. H., and Baldwin, R. L. (1993) *Biochemistry 32*, 9668−9676.
18. Armstrong, K. M., and Baldwin, R. L. (1993) *Proc. Natl. Acad. Sci. U.S.A. 90*, 11337−11340.
19. Doig, A. J., Charkrabartty, A., Klinger, T. M., and Baldwin, R. L. (1994) *Biochemistry 33*, 3396−3403.
20. Doig, A. J., and Baldwin, R. L. (1995) *Protein Sci. 4*, 1325−1336.
21. Johnson, M. J. (1983) *Biophys. J. 44*, 101−106.
22. Johnson, M. J., and Frasier, S. G. (1985) *Methods Enzymol. 117*, 301−342.
23. Marqusee, S., Robbins, V. H., and Baldwin, R. L. (1989) *Proc. Natl. Acad. Sci. U.S.A. 86*, 5286−5290.
24. Scholtz, J. M., Marqusee, S., Baldwin, R. L., York, E. J., Stewart, J. M., Santoro, M., and Bolen, D. W. (1991) *Proc. Natl. Acad. Sci. U.S.A. 88*, 2854−2858.
25. Chakrabartty, A., Schellman, J. A., and Baldwin, R. L. (1991) *Nature 351*, 586−588.
26. Rohl, C. A., Scholtz, J. M., York, E. J., Stewart, J. M., and Baldwin, R. L. (1992) *Biochemistry 31*, 1263−1269.
27. Scholtz, J. M., and Baldwin, R. L. (1992) *Annu. Rev. Biophys. Biomol. Struct. 21*, 95−118.
28. Shalongo, W., Dugad, L., and Stellwagen, E. (1994) *J. Am. Chem. Soc. 116*, 8288−8293.
29. Shalongo, W., Dugad, L., and Stellwagen, E. (1994) *J. Am. Chem. Soc. 116*, 2500−2507.
30. Scholtz, J. M., Barrick, D., York, E. J., Stewart, J. M., and Baldwin, R. L. (1995) *Proc. Natl. Acad. Sci. U.S.A. 92*, 185−189.
31. Shalongo, W., and Stellwagen, E. (1995) *Protein Sci. 4*, 1161−1166.
32. Chakrabartty, A., Kortemme, T., and Baldwin, R. L. (1994) *Protein Sci. 3*, 843−852.
33. Myers, J. K., Pace, C. N., and Scholtz, J. M. (1997) *Proc. Natl. Acad. Sci. U.S.A. 94*, 2833−2837.
34. Myers, J. K., Pace, C. N., and Scholtz, J. M. (1997) *Biochemistry 36*, 10923−10929.
35. Marqusee, S., and Baldwin, R. L. (1987) *Proc. Natl. Acad. Sci. U.S.A. 84*, 8898−8902.
36. Gans, P. J., Lyu, P. C., Manning, M. C., Woody, R. W., and Kallenbach, N. R. (1991) *Biopolymers 31*, 1605−1614.
37. Merutka, G., and Stellwagen, E. (1991) *Biochemistry 30*, 1591−1594.
38. Huyghues-Despointes, B. M. P., Scholtz, J. M., and Baldwin, R. L. (1993) *Protein Sci. 2*, 80−85.
39. Blasie, C. A., and Berg, J. M. (1997) *Biochemistry 36*, 6218−6222.
40. Myers, J. K., and Pace, C. N. (1996) *Biophys. J. 71*, 2033−2039.
41. Honig, B., and Yang, A. S. (1995) *Adv. Protein Chem. 46*, 27−58.
42. Lazaridis, T., Archontis, G., and Karplus, M. (1995) *Adv. Protein Chem. 47*, 231−306.

BI972026H